IEEE Access
Multidisciplinary ⋮ Rapid Review ⋮ Open Access Journal

Received September 3, 2020, accepted September 14, 2020, date of publication September 18, 2020,
date of current version September 30, 2020.

Digital Object Identifier 10.1109/ACCESS.2020.3025146

A Comparison of One- and Two-Diode Model Parameters at Indoor Illumination Levels

SEBASTIAN BADER, (Senior Member, IEEE), XINYU MA, (Student Member, IEEE), AND BENGT OELMANN
Department of Electronics Design, Mid Sweden University, 85170 Sundsvall, Sweden
Corresponding author: Sebastian Bader (sebastian.bader@miun.se)

ABSTRACT Indoor photovoltaic (PV) application gains in attraction for low-power electronic systems, which requires accurate methods for performance predictions in indoor environments. Despite this, the knowledge on the performance of commonly used photovoltaic device models and their parameter estimation techniques in these scenarios is very limited. Accurate models are an essential tool for conducting feasibility analyses and component dimensioning for indoor photovoltaic systems. In this paper, we therefore conduct a comparison of the one- and two-diode models with parameters estimated based on two well-known methods. We evaluate the models' performance on datasets of photovoltaic panels intended for indoor use, and illumination conditions to be expected in indoor environments lit by artificial light sources. The results demonstrate that the one-diode model outperforms the two-diode model with respect to the estimation of the overall I-V characteristics. The two-diode model results instead in lower maximum power point errors. Both models show a sensitivity to initial conditions, such as the selection of the diode ideality factor, as well as the curve form of the photovoltaic panel to be modeled, which has not been acknowledged in previous research.

INDEX TERMS Indoor photovoltaics, energy harvesting, photovoltaic cell models, one-diode model, two-diode model, parameter estimation.

I. INTRODUCTION

Models of photovoltaic (PV) devices are an essential tool for the estimation of the devices' I-V and P-V characteristics. These, in turn, are essential to estimate the output power of PV devices under different application conditions. In the majority of cases, such models are based on equivalent circuits, amongst which the one-diode and two-diode models have gained highest popularity [1]–[4]. In these models, the pn-junction behavior of the PV cells is modeled with one or two lumped diodes, and losses are considered through the inclusion of series and parallel resistances.

In order to implement the model for a specific PV device, a number of circuit parameters need to be estimated. Due to the nonlinear and implicit nature of the models' governing equations, the parameter estimation problem is recognized to be challenging, and innumerous parameter estimation methods have been proposed in the scientific literature [2], [4]. The parameter estimation methods use data supplied by the manufacturer, or measured data, to estimate the model parameters. Their approaches can be categorized into being analytical, numerical/iterative, or metaheuristic [3], [4].

Traditionally, the parameter estimation methods were developed and investigated under outdoor conditions with irradiance levels of about $200\,\mathrm{W\,m^{-2}}$ to $1000\,\mathrm{W\,m^{-2}}$. However, the usage of PV devices in indoor scenarios increases with the growing availability of low-power electronic systems [5]–[7]. At the same time, there is a limited number of studies on the performance of parameter estimation methods under indoor illumination conditions [8]–[12]. These conditions are commonly defined by much lower light intensities (i.e. $<10\,\mathrm{W\,m^{-2}}$), and have different light spectra [13]–[16]. While the two-diode model has been shown to have superior performance in outdoor conditions, conflicting results on its performance have been presented in some of previous studies. For instance, results presented by Masoudinejad *et al.* [9] demonstrated lower performance of the two-diode model when compared to the one-diode model. Moreover, differences in the effects on PV cell performances and losses in indoor lighting conditions have been

The associate editor coordinating the review of this manuscript and approving it for publication was Wen-Sheng Zhao.

shown [17], [18]. The limitation in studies on parameter estimation methods under low light conditions poses a knowledge gap on the performance of common PV models and their parameter estimation methods in such situations. This knowledge gap limits the ability to estimate PV device operation and estimate output power under indoor illumination conditions.

The goal of this paper is to systematically compare two popular parameter estimation methods at indoor illumination levels. The two selected methods of Villalva *et al.* [19] and Ishaque *et al.* [20] apply the same iterative approach on the one- and two-diode models, and are therefore a good basis for the intended comparison. The methods are frequently used in the community for parameter estimations under outdoor conditions, but have not previously been compared under low illumination levels. Both methods are applied to two typical PV panel choices for indoor applications, based on amorphous and crystalline silicon, respectively.

We evaluate each method in regard to its parameter estimation performance at different illumination levels, as well as the effects of scaling the estimated parameters to other illumination conditions. The comparison demonstrates that the implemented models behave considerably different, and that an expected performance benefit of the two-diode model is not observed when using the chosen parameter estimation techniques. Instead the physical advantage of the two-diode model appears to be limited by restrictions of the parameter estimation method applied. The study, moreover, highlights that the selection of the diode ideality factor, which is often neglected, has significant performance effects and can be utilized to fine tune the model performance.

The remainder of this paper is organized as follows. In Section II, we summarize the one-diode and two-diode models, followed by a presentation of the used parameter estimation methods in Section III. Section IV provides information on the data acquisition and evaluation metrics. In Section V, we present and discuss the obtained results, and finally we conclude the article in Section VI.

II. EQUIVALENT CIRCUIT MODELS

Equivalent circuit models are commonly used to describe the I-V characteristics of PV devices. Fig. 1 depicts the equivalent circuit diagrams of the one- and two-diode models.

A. ONE-DIODE MODEL

The one-diode model (or single-diode model) is the most popular model for PV devices. It models the PV device as a current source, a diode, and two resistors, as depicted in Fig. 1a. Based on circuit analysis, the relationship between the current I and voltage V can be mathematically described as

$$I = I_{pv} - I_0\left[exp\left(\frac{V + R_s I}{nN_s V_t}\right) - 1\right] - \frac{V + R_s I}{R_{sh}}. \quad (1)$$

Herein, I_{pv} denotes the photocurrent, I_0 the diode reverse saturation current, n the diode ideality factor, N_s the number of PV cells connected in series, R_s the series resistance, and

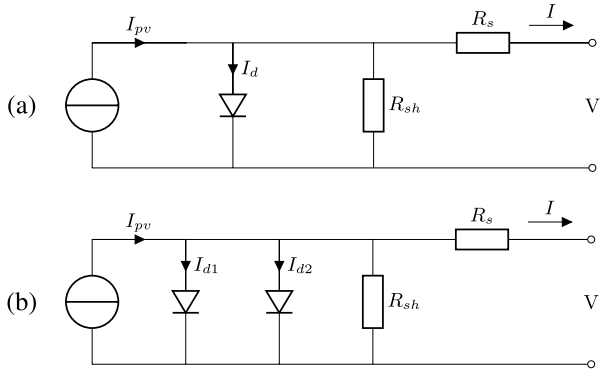

FIGURE 1. Equivalent circuit diagrams of the (a) one-diode model and (b) two-diode model.

R_{sh} the shunt (or parallel) resistance. Moreover, V_t is the thermal voltage with

$$V_t = \frac{kT}{q}, \quad (2)$$

where k is the Boltzmann constant, T the absolute temperature of the pn-junction, and q is the electron charge.

The model has five unknown parameters, namely I_{pv}, I_0, n, R_s and R_{sh}. These parameters are commonly not provided by PV device manufacturers, and it is the aim of the parameter estimation method to determine accurate values based on available data.

B. TWO-DIODE MODEL

The two-diode model is very similar to the one-diode model, but includes a second diode in parallel to the current source. The equivalent circuit of the model is depicted in Fig. 1b. The second diode is particularly envisaged to represent the recombination losses in the depletion region [21]. Its I-V relationship can be described accordingly as

$$I = I_{pv} - I_{01}\left[exp\left(\frac{V + R_s I}{n_1 N_s V_t}\right) - 1\right] - I_{02}\left[exp\left(\frac{V + R_s I}{n_2 N_s V_t}\right) - 1\right] - \frac{V + R_s I}{R_{sh}}. \quad (3)$$

Equation (3) contains two diode-related terms, with I_{01} and I_{02} denoting the reverse saturation currents and n_1 and n_2 denoting the diode ideality factors, respectively.

Due to the second diode, the two-diode model allows to achieve greater accuracy, and is commonly related to better performance at lower irradiance levels [1], [3], [22]. On the other hand, the model has seven unknown parameters (I_{pv}, I_{01}, I_{02}, n_1, n_2, R_s, R_{sh}), which increases the complexity of the parameter estimation problem. In order to simplify the parameter estimation, it is therefore common to assume some of the model parameters to be constant.

III. PARAMETER ESTIMATION METHODS

For the comparison in this study, the parameter estimation methods of Villalva *et al.* [19] and Ishaque *et al.* [20] have been selected. The two methods use the same approach for

the parameter estimation, but are adjusted for the one- and two-diode model, respectively.

A. METHOD OF VILLALVA *et al.*

Villalva *et al.* [19] proposed an iterative method for the estimation of the one-diode model parameters. The method iterates through a range of R_s values and calculates the remaining dependent parameters analytically. For each set of model parameters, the maximum power P_{max} is estimated and compared to the power at the true maximum power point (MPP).

The method is initiated by determining values for n and I_0. The diode ideality factor n can according to the authors be arbitrarily chosen, but it is mentioned that typical choices lie in the value range $1 \leq n \leq 1.5$. I_0 is then determined according to

$$I_0 = \frac{I_{sc} + K_I \Delta T}{exp((V_{oc} + K_V \Delta T)/nV_t) - 1}, \tag{4}$$

where V_{oc} is the open-circuit voltage, I_{sc} is the short-circuit current, and K_I, K_V are the current and voltage coefficients of the PV device, describing its temperature dependency.

Afterwards, the series resistance is initiated as $R_s = 0$ and then incremented iteratively. For each value of R_s, the shunt resistance R_{sh} is estimated as

$$R_{sh} = \frac{(V_{mp} + I_{mp}R_s)}{I_{pv} - I_0\, exp\left[\frac{(V_{mp}+I_{mp}R_s)}{nN_sV_t}\right] + I_0 - I_{mp}}, \tag{5}$$

where V_{mp} and I_{mp} are the voltage and current at the point of maximum power extraction. Furthermore, I_{pv} is estimated according to

$$I_{pv} = \frac{R_{sh} + R_s}{R_{sh}} I_{sc}. \tag{6}$$

With this, the estimation method results in a set of parameters that minimizes the MPP error for a given R_s-range and value of n. These parameters can therefore be tuned to further improve the model parameters. The parameter estimation process is summarized in the flowchart depicted in Fig. 2a.

B. METHOD OF ISHAQUE *et al.*

Ishaque *et al.* [20] adapted the previously described method to the two-diode model. The overall approach of the proposed method is identical and thus bases on the iteration of R_s and evaluation of the MPP error. In order for this method to be applicable, Ishaque *et al.* reduce the parameter set of the two-diode model based on a number of simplifying assumptions. The overall process is visualized in Fig. 2b.

Similarly to [19], the diode ideality factors n_1 and n_2 are initiated with constant values. The method prescribes $n_1 = 1$, which is motivated based on Shockley's diffusion theory [21], but allows n_2 to be freely selected. The authors recommend a value of $n_2 \geq 1.2$, and a value of $n_2 = 2$ is a common value in the research community.

The method, moreover, initiates the reverse saturation currents of the two diodes to be of the same magnitude, and their

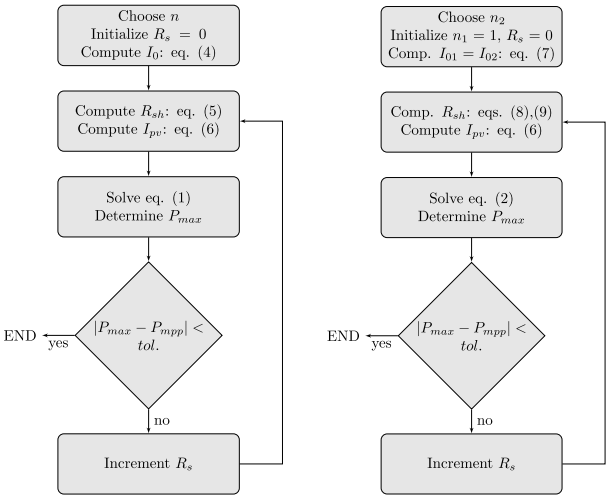

(a) Villalva *et al.* (b) Ishaque *et al.*

FIGURE 2. Flowcharts of the the parameter estimation methods of (a) Villalva *et al.* for the one-diode model and (b) Ishaque *et al.* for the two-diode model.

value can be estimated according to

$$I_{0x} = \frac{I_{sc} + K_i \Delta T}{exp[(V_{oc} + K_v \Delta T)/V_t] - 1}. \tag{7}$$

Based on these initial values, R_s is incremented iteratively, and R_{sh} and I_{pv} are estimated for each value of R_s. For this, R_{sh} is based on

$$R_{sh} = \frac{V_{mp} + I_{mp}R_s}{I_{pv} - I_{d1} - I_{d2} - I_{mp}}, \tag{8}$$

where

$$I_{dx} = I_{0x}\left[exp\left(\frac{V_{mp} + I_{mp}R_s}{n_x V_t}\right) - 1\right]. \tag{9}$$

The estimation of I_{pv} is based on (6).

As a result, a set of model parameters optimized for a low MPP error is obtained. Similarly to the method of Villalva *et al.*, n_2 and the R_s value range can be used to further optimize the results.

IV. DATASET AND EVALUATION APPROACH

The comparison in this study is based on model evaluation with estimated parameters under identical conditions. The overall approach for this evaluation is as follows. Based on experimentally obtained I-V characteristics, the model parameters of the one- and two-diode models were estimated following the methods of Villalva *et al.* [19] and Ishaque *et al.* [20], respectively.

Both parameter estimation methods have been implemented as MATLAB® functions, returning the set of model parameters for the respective model based on the specific input parameters. The required input parameters are the R_s value range to be evaluated, the n or n_2 value for the estimation run, as well as the remarkable points of the I-V characteristic to be modeled (i.e. V_{oc}, I_{sc}, V_{mp} and I_{mp}). The R_s value range was selected for each illumination condition to

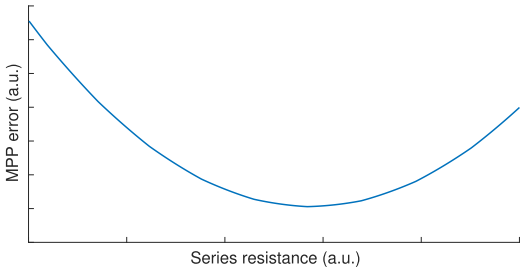

FIGURE 3. Illustrative example of the result of an R_S-sweep during parameter estimation. The value range for R_S needs to be selected to include the minimum MPP error.

TABLE 1. PV panel parameters (at STC).

Symbol	Description	IXYS	Sanyo
N	Number of cells	10	6
A	Panel size	7.7 cm^2	5 cm^2
V_{oc}	Open circuit voltage	6.3 V	5.1 V
I_{sc}	Short circuit current	25 mA	5.1 mA
V_{mp}	Maximum power point voltage	5.01 V	3.9 V
I_{mp}	Maximum power point current	22.3 mA	4.6 mA

include the minimum MPP error, which was verified through visual inspection. An example R_s-sweep is depicted in Fig. 3. Parameter estimations were repeated for different diode ideality factors, with $1 \leq n \leq 10$ and $1.2 \leq n_2 \leq 10$ with increments of 0.1.

A dataset of I-V characteristics was created experimentally. The same dataset was used to extract the remarkable points for parameter estimation, as well as to evaluate the resulting models. The dataset contains I-V characteristics for two PV panels, namely an IXYS SLMD600H10L panel based on 10 crystalline silicon cells, and a Sanyo AM5610 panel based on 6 amorphous silicon cells. Both panels are common PV devices for indoor application scenarios, and their key properties are listed in Table 1. They differ significantly in form-factor and rated output from large-scale PV panels commonly used in outdoor solar applications. For each panel, I-V characteristics were obtained from 100 lx to 1000 lx in increments of 100 lx. The illumination conditions were generated by LED light with a color temperature of 2700 K, and verified by an AMS TSL2561 ambient light sensor. In contrast to typical outoor conditions (e.g. Standard Test Conditions with 1000 W m^{-2}, 25 °C, and AM1.5), most artificial light sources are restricted to the human visible light spectrum (approx. 380 nm to 740 nm). The I-V characteristics themselves were obtained with a Keysight B2901 source-measure unit with a voltage step-size of 3 mV. The temperature of the PV panels was maintained constant at approximately 25 °C during data collection.

Each model was evaluated against the experimental I-V characteristics in the dataset. For this, the estimated model parameters were used to predict the I-V curve under a given illumination condition, which was then compared to the true curve from the dataset. As metrics for the evaluations the

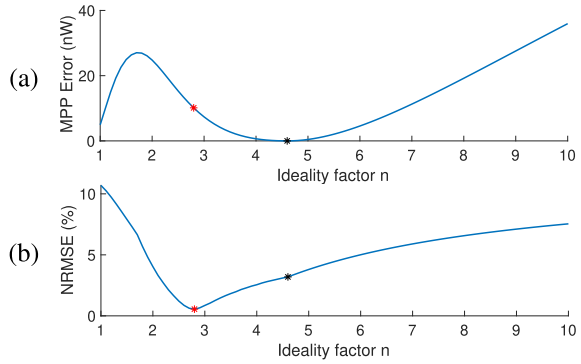

FIGURE 4. Influence of n value on the performance of the one-diode model with parameter estimation according to Villalva *et al.* Example depicts results for the crystalline panel at 100lx.

MPP error (MPPE) and the normalized root mean squared error (NRMSE) was utilized. For the NRMSE, the RMS error of the I-V curves was normalized with the short-circuit current, such that

$$\mathrm{NRMSE}\,(\%) = \frac{100}{I_{sc}} \cdot \sqrt{\frac{1}{k}\sum_{i=1}^{k}\left(I_i^{mod} - I_i^{exp}\right)^2}. \qquad (10)$$

Here, I_i^{mod} and I_i^{exp} are the i^{th} modeled and experimental current value in the respective datasets of length k. These two metrics evaluate a single operating point (MPPE) and the reproduction of the overall I-V curve shape (NRMSE), respectively.

Each model, moreover, was evaluated with respect to the effects of scaling the estimated parameters to different illumination conditions. For this, the model parameters estimated at 1000 lx were scaled to the other illumination conditions. The effects were evaluated based on the previously mentioned metrics. Different approaches for the scaling of the model parameters have been reported in the scientific literature. All these approaches have in common that they include a linear illumination-dependency of the photocurrent. However, it is argued upon whether the shunt resistance R_{sh} also should be scaled with illumination. Different such methods have been reported, including linear [23], exponential [24], and power-law [8] scaling. For the comparison in this study, each scaling method was applied and the respective results were compared with each other.

V. RESULTS

The results for each model after successful parameter estimation are presented individually, followed by a discussion and comparison.

A. ONE-DIODE MODEL

Fig. 4 depicts a representative result for sweeping the diode ideality factor n in the parameter estimation method according to Villalva *et al.* [19]. This example result relates to a specific test condition, which in this case is an illumination level of 100 lx and the modeling of the crystalline PV panel. The result shows a clear dependency of the model's performance

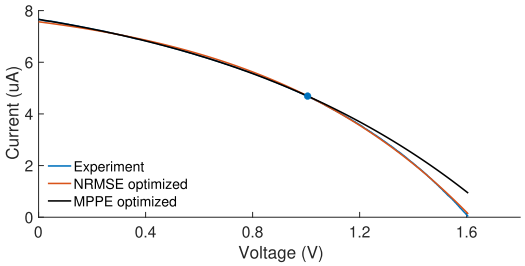

FIGURE 5. Comparison of measured and modeled I-V curves for the crystalline panel at 100lx. Modeled I-V curves are estimated based on Villalva *et al.*

on the chosen ideality factor. Although this dependency exists for both the MPPE and the NRMSE, the MPPE is over the entire range of n of negligible magnitude. In contrast, significant differences in the NRMSE are observed. Consequently, the selection of the value of n becomes significant for the model performance, as it results in different model parameters.

In Fig. 4 two potential choices for the value of n are indicated. These are the values that minimize MPPE (black marker) or NRMSE (red marker), respectively. As it can be seen in the figure, each choice will influence the performance of the model with respect to the respective other metric as well. Optimizing for MPPE will result in an MPPE of 7.08e–13 W and an NRMSE of 3.19 %, whereas an optimization for NRMSE results in an MPPE of 1.01e–8 W and an NRMSE of 0.55 %. Due to the larger impact on NRMSE, the value of n that optimizes NRMSE appears to be the better alternative.

This is confirmed when investigating the resulting I-V curve estimates of the two sets of model parameters, which are depicted in Fig. 5. It can be seen that the model based on the NRMSE optimized value for n results in an I-V curve that has an overall better match with the experiment than when optimizing for the MPPE. The MPPE optimized parameters particularly lead to estimation errors close to V_{oc}, which can be observed consistently for all illumination levels. Nonetheless, both sets of parameters result in an accurate prediction at the maximum power point (blue marker).

Similar observations have also been made for the amorphous PV panel. However, the model generally produced a worse fit for the I-V curves of the amorphous PV panel, which results in a larger NRMSE. The model, nonetheless, profits from selecting n based on NRMSE minimization even in this case.

Fig. 6 illustrates the effect of model parameter scaling for one case of the crystalline and amorphous PV panels, respectively. In these cases, the model parameters have first been estimated for an illumination level of 1000 lx (NRMSE optimized n). Afterwards, the I-V curves for the other illumination levels have been estimated by scaling I_{pv} and R_{sh} of the estimated parameter set. The results for the crystalline panel (Fig. 6a) shows that the I-V curves based on scaled parameters demonstrate, in most cases, a good fit with experiment. Generally, the match worsens, and the NRMSE increases, with scaling to conditions further from the reference, i.e. lower illumination levels. Different scaling approaches for R_{sh} have been evaluated (cf. Section IV). For the crystalline panel no significant difference was observed, and the results shown in Fig. 6a neglect scaling of R_{sh}.

For the amorphous PV panel (Fig. 6b), the results show a worse match between estimated and experimental I-V curves. Already the initially estimated parameters (1000 lx) result in a mismatch between the curve form of the model and experiment. This mismatch remains when scaling the parameters to other conditions, which suggests the importance of a good initial curve match. The models result in considerable errors, particularly in the region close to the open-circuit voltage. Similar to the crystalline panel, an increasing NRMSE with decreasing illumination is observed. Scaling of R_{sh} showed an improvement in estimation performance, but no significant effect was observed for different scaling methods of R_{sh}.

B. TWO-DIODE MODEL

Fig. 7 depicts an example result for the effect of sweeping the diode ideality factor n_2 in the parameter estimation method according to Ishaque *et al.* [20]. The results show that there is little effect on the MPPE, and that influences on the NRMSE diminishes quickly after an initial drop. As a result, any value above a certain threshold may be chosen, and the value selection for n_2 is much less sensitive than for the one-diode model. For all cases evaluated in this studies, however, values of $n_2 < 2$ should be avoided. In particular, the minimum value of $n_2 = 1.2$, suggested by the authors in [20], resulted in large NRMSEs.

In the same manner as for the one-diode model, two n_2 values have been evaluated further, optimizing for MPPE and NRMSE, respectively. Although these optimizations resulted in several cases in considerably different values of n_2, the performance of the resulting set of parameters was largely unaffected. In the example given in Fig. 7, optimization for MPPE resulted in an MPPE of 4.28e–16 W and an NRMSE of 3.85 %, whereas an NRMSE optimized value for n_2 resulted in an MPPE of 8.07e–13 W and an RMSE of 3.78 %.

This performance similarity is also shown in the respective I-V curve example depicted in Fig. 8. The I-V curves of the two sets of parameters are almost identical and visually not separable. In this case both model implementations, however, underestimate the output current at voltages above V_{mp}.

With respect to parameter scaling, Fig. 9 depicts the result of the scaling for the estimated parameters of the two-diode model. In the same manner as for the one-diode model, the parameters are first estimated at an illumination of 1000 lx, and then the I-V curve of the other illumination conditions are estimated based on the scaling of I_{pv} and R_{sh}. The results show significant deviations of the estimated I-V curves in comparison from the measured curves. This is true for both the crystalline panel (Fig. 9a) and the amorphous panel (Fig. 9b). However, the errors in estimating the behavior of the amorphous panel is again significantly larger than those of the crystalline panel. In both cases, mismatches of

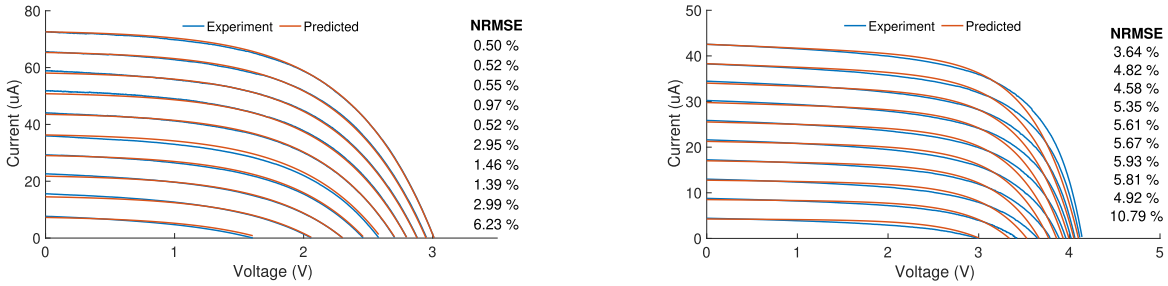

(a) Crystalline panel (b) Amorphous panel

FIGURE 6. Performance of scaled parameter sets for the one-diode model parameters. Performance is depicted for (a) the crystalline PV panel and (b) the amorphous PV panel.

TABLE 2. Summary of performance results for parameter estimation at different illumination conditions.

Illumination condition (lx)	One-diode (Villalva)				Two-diode (Ishaque)			
	Crystalline (Ixys)		Amorphous (Sanyo)		Crystalline (Ixys)		Amorphous (Sanyo)	
	MPPE (W)	NRMSE (%)	MPPE (W)	NRMSE (%)	MPPE (W)	NRMSE (%)	MPPE (W)	NRMSE (%)
100	1.01e−8	0.55	1.08e−7	3.65	4.96e−9	10.70	3.56e−14	3.76
200	8.56e−9	0.75	2.55e−7	2.76	3.12e−10	5.40	1.13e−12	3.90
300	5.85e−10	0.93	1.88e−7	2.62	8.07e−13	3.78	2.38e−12	4.19
400	3.04e−11	0.75	4.09e−8	2.55	9.35e−13	3.43	3.61e−12	4.63
500	7.81e−8	1.05	3.86e−7	2.86	1.96e−13	3.81	5.46e−12	4.58
600	2.21e−8	0.71	3.96e−7	3.37	1.09e−13	3.31	2.54e−12	4.95
700	2.35e−8	0.73	6.71e−7	3.43	4.33e−13	3.28	8.38e−12	4.88
800	3.60e−8	0.72	4.90e−7	3.50	1.29e−13	2.98	2.56e−12	5.10
900	3.33e−10	0.50	5.84e−7	3.57	4.50e−13	2.91	4.04e−12	5.17
1000	8.94e−9	0.50	1.67e−9	3.65	1.15e−12	2.80	1.83e−12	5.92

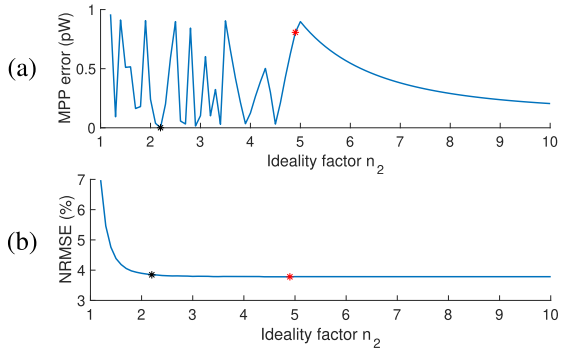

FIGURE 7. Effect of n_2 on the model performance of the two-diode model with parameter estimation according to Ishaque *et al.* Example depicts results for the crystalline panel at 300lx.

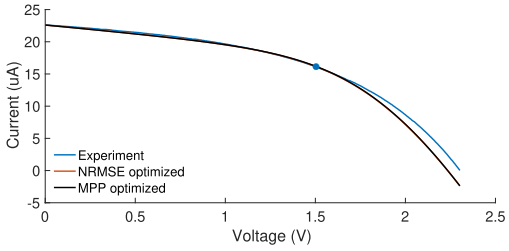

FIGURE 8. Comparison of measured and modeled I-V curves for the crystalline panel at 300lx. Modeled I-V curves are estimated based on Ishaque *et al.*

the modeled and measured I-V curve already exist in the reference conditions (i.e. initial parameter estimation).

C. DISCUSSION AND COMPARISON

The results presented in the previous sections show considerable differences between the one- and two-diode models with parameters estimated according to the evaluated methods. This concerns both their behavior (i.e. sensitivity to input parameters such as the diode ideality factor), as well as the performance of the resulting model implementations.

Table 2 summarizes the performance results of the implemented one- and two-diode models for all combinations of PV panels and illumination conditions. For each condition, the MPPE and NRMSE are provided. The results show that the one-diode model accurately estimated the performance for the crystalline PV panel, whereas it resulted in larger errors for the amorphous panel. In particular, the voltage region between V_{mp} and V_{oc} demonstrated a clear mismatch between modeled and measured I-V curves. For the two-diode model, the modeling of both PV panels resulted in clear deviations from the measured curve forms, and thus relatively high NRMSE values. For both models, the modeling of the crystalline panel generally produced a more accurate result than the amorphous panel model. An exception are very low illumination levels for the two-diode model (i.e. 100 lx and 200 lx), where a high NRMSE for the crystalline panel is observed.

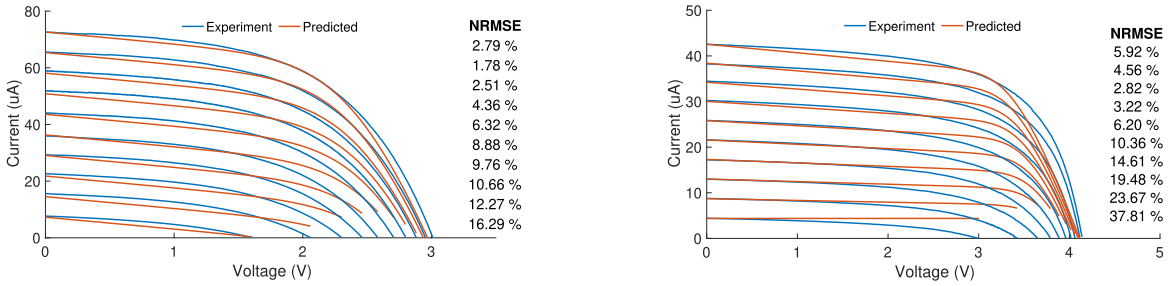

(a) Crystalline panel (b) Amorphous panel

FIGURE 9. **Performance of scaled parameter sets of the two-diode model. Performance is depicted for (a) the crystalline PV panel and (b) the amorphous PV panel.**

Comparing the results of the one-diode and two-diode models, it can be observed that the one-diode model results in a better I-V curve match. This is shown in Table 2 through lower NRMSE values for all illumination conditions. On the other hand, the two-diode model results in considerable lower MPPEs, and less variation in MPPEs. Although the MPPEs of the two-diode model are in most cases several orders of magnitude lower than the respective error for the one-diode model, it may be argued that the error in all cases is sufficiently low. The largest MPPE for the one-diode model, for example, is 6.71e–7 W, obtained at 700 lx for the amorphous PV panel. With a maximum power of 72.69 μW under this condition, the relative MPPE is only 0.92 %.

Also for parameter scaling, a better result of the I-V curve form was observed for the one-diode model. Here, the curve match of the reference condition (i.e. the condition the parameters have been initially estimated for) plays a crucial role in scaling performance. While the scaling of R_{sh} could compensate in some cases for the initial curve mismatch, leading to minor scaling improvements, the selection of different scaling approaches showed little effect on the overall performance.

VI. CONCLUSION

The results in this paper demonstrate considerable differences between the performances of the two models implemented based on the selected parameter estimation techniques. Although the two-diode model is known to be more accurate in outdoor irradiance conditions, its overall performance was observed to be worse under the evaluated indoor conditions. While the two-diode model leads to more accurate estimations of the maximum power point, the significance of this improvement is negligible, as all MPPEs were low relative to the MPP. With NRMSE differences demonstrating a clear effect on I-V curve match, it can therefore be concluded that the one-diode model with parameter estimation based on Villalva *et al.* [19] is the preferable choice for the evaluated indoor conditions.

A likely explanation for this is that the two-diode model provides additional degrees of freedom. The set of model parameters can therefore be selected by the parameter estimation model to optimize its key metric, which in this case is a matching maximum power point. However, this comes at a potential cost of an overall mismatching curve shape, i.e. the method overfits the result for a single operating point. The performance results therefore show an improved MPPE, but an increased NRMSE. It can therefore be concluded that the higher general performance of the two-diode model is limited by the restrictions of the applied parameter estimation method.

It was, moreover, observed that the modeling of different PV panels leads to considerably different performance results. Modeling of the crystalline PV panel demonstrated in most cases better accuracy than those of the amorphous PV panel. This leads to the conclusion that the investigated modeling methods are sensitive to the I-V curve form of the PV panels to be modeled. However, with a limited number of panels investigated, it is difficult to conclude whether the performance can be linked to specific PV technologies. Investigations on a larger set of devices are desirable.

Furthermore, a performance dependency on the diode ideality factor was observed. While related works suggest arbitrary selection of these parameters, or recommend constant values, our results suggest that the selection may have significant effects on model performance. In the presented study, this was particularly the case for the one-diode model with parameter estimations according to Villalva *et al.* From the comparison of two alternative selection criteria, we can conclude that a parameter selection aiming at NRMSE optimization is preferable if an overall match of the I-V curve form is targeted. Consequently, the diode ideality factor selection can be used to regain some control over the parameter estimation method, and to fine-tune the performance of the resulting models.

Overall, considerable errors were observed in the models' performance under indoor illumination conditions. With indoor photovoltaic solutions gaining in application, this poses a challenge for accurate performance estimations. This is in agreement with previous studies that have demonstrated different cell behaviors, efficiencies and losses when operated under indoor illumination conditions [17], [18]. Additional work on the improvement of parameter estimation methods or entirely new models for indoor photovoltaic conditions are therefore needed.

REFERENCES

[1] V. J. Chin, Z. Salam, and K. Ishaque, "Cell modelling and model parameters estimation techniques for photovoltaic simulator application: A review," *Appl. Energy*, vol. 154, pp. 500–519, Sep. 2015.
[2] A. M. Humada, M. Hojabri, S. Mekhilef, and H. M. Hamada, "Solar cell parameters extraction based on single and double-diode models: A review," *Renew. Sustain. Energy Rev.*, vol. 56, pp. 494–509, Apr. 2016.
[3] A. R. Jordehi, "Parameter estimation of solar photovoltaic (PV) cells: A review," *Renew. Sustain. Energy Rev.*, vol. 61, pp. 354–371, Aug. 2016.
[4] R. Abbassi, A. Abbassi, M. Jemli, and S. Chebbi, "Identification of unknown parameters of solar cell models: A comprehensive overview of available approaches," *Renew. Sustain. Energy Rev.*, vol. 90, pp. 453–474, Jul. 2018.
[5] G. Apostolou, A. Reinders, and M. Verwaal, "Comparison of the indoor performance of 12 commercial PV products by a simple model," *Energy Sci. Eng.*, vol. 4, no. 1, pp. 69–85, Jan. 2016.
[6] I. Mathews, P. J. King, F. Stafford, and R. Frizzell, "Performance of III–V solar cells as indoor light energy harvesters," *IEEE J. Photovolt.*, vol. 6, no. 1, pp. 230–235, Jan. 2016.
[7] P. Spachos and A. Mackey, "Energy efficiency and accuracy of solar powered BLE beacons," *Comput. Commun.*, vol. 119, pp. 94–100, Apr. 2018.
[8] N. F. Tinsley, S. T. Witts, J. M. R. Ansell, E. Barnes, S. M. Jenkins, D. Raveendran, G. V. Merrett, and A. S. Weddell, "Enspect: A complete tool using modeling and real data to assist the design of energy harvesting systems," in *Proc. 3rd Int. Workshop Energy Harvesting Energy Neutral Sens. Syst.*, 2015, pp. 27–32.
[9] M. Masoudinejad, M. Kamat, J. Emmerich, M. ten Hompel, and S. Sardesai, "A gray box modeling of a photovoltaic cell under low illumination in materials handling application," in *Proc. 3rd Int. Renew. Sustain. Energy Conf. (IRSEC)*, Dec. 2015, pp. 1–6.
[10] A. Fajardo Jaimes and F. Rangel de Sousa, "Simple modeling of photovoltaic solar cells for indoor harvesting applications," *Sol. Energy*, vol. 157, pp. 792–802, Nov. 2017.
[11] S. Bader, X. Ma, and B. Oelmann, "One-diode photovoltaic model parameters at indoor illumination levels—A comparison," *Sol. Energy*, vol. 180, pp. 707–716, Mar. 2019.
[12] X. Ma, S. Bader, and B. Oelmann, "A scalable, data-driven approach for power estimation of photovoltaic devices under indoor conditions," in *Proc. 7th Int. Workshop Energy Harvesting Energy-Neutral Sens. Syst.*, 2019, pp. 29–34.
[13] B. Minnaert and P. Veelaert, "A proposal for typical artificial light sources for the characterization of indoor photovoltaic applications," *Energies*, vol. 7, no. 3, pp. 1500–1516, Mar. 2014.
[14] Y. Li, N. J. Grabham, S. P. Beeby, and M. J. Tudor, "The effect of the type of illumination on the energy harvesting performance of solar cells," *Sol. Energy*, vol. 111, pp. 21–29, Jan. 2015.
[15] X. Ma, S. Bader, and B. Oelmann, "Characterization of indoor light conditions by light source classification," *IEEE Sensors J.*, vol. 17, no. 12, pp. 3884–3891, Jun. 2017.
[16] X. Ma, S. Bader, and B. Oelmann, "Power estimation for indoor light energy harvesting systems," *IEEE Trans. Instrum. Meas.*, vol. 69, no. 10, pp. 7513–7521, Oct. 2020.
[17] K. Ruhle, M. Freunek, L. M. Reindl, and M. Kasemann, "Designing photovoltaic cells for indoor energy harvesting systems," in *Proc. Int. Multi-Conf. Syst., Sygnals Devices*, Mar. 2012, pp. 1–5.
[18] B. H. Hamadani, "Understanding photovoltaic energy losses under indoor lighting conditions," *Appl. Phys. Lett.*, vol. 117, no. 4, Jul. 2020, Art. no. 043904.
[19] M. G. Villalva, J. R. Gazoli, and E. R. Filho, "Comprehensive approach to modeling and simulation of photovoltaic arrays," *IEEE Trans. Power Electron.*, vol. 24, no. 5, pp. 1198–1208, May 2009.
[20] K. Ishaque, Z. Salam, and H. Taheri, "Simple, fast and accurate two-diode model for photovoltaic modules," *Sol. Energy Mater. Sol. Cells*, vol. 95, no. 2, pp. 586–594, Feb. 2011.
[21] C.-T. Sah, R. Noyce, and W. Shockley, "Carrier generation and recombination in P-N junctions and P-N junction characteristics," *Proc. IRE*, vol. 45, no. 9, pp. 1228–1243, Sep. 1957.
[22] S. Bana and R. P. Saini, "A mathematical modeling framework to evaluate the performance of single diode and double diode based SPV systems," *Energy Rep.*, vol. 2, pp. 171–187, Nov. 2016.
[23] W. De Soto, S. A. Klein, and W. A. Beckman, "Improvement and validation of a model for photovoltaic array performance," *Sol. Energy*, vol. 80, no. 1, pp. 78–88, Jan. 2006.
[24] PVSyst. *PV Module—Rshunt Exponential Behavior Irradiance*. Accessed: Sep. 3, 2020. [Online]. Available: https://www.pvsyst.com/help/pvmodule_rshexp.htm

SEBASTIAN BADER (Senior Member, IEEE) received the Ph.D. degree in electronics from Mid Sweden University, Sundsvall, Sweden, in 2013, and the Dipl.Ing. degree from the University of Applied Sciences, Wilhelmshaven, Germany. He is currently an Assistant Professor of electronics engineering with the Department of Electronics Design, Mid Sweden University. His research interests include energy harvesting, networked embedded systems, low-power sensor systems and their applications, energy transducer design, and optimization and modeling, as well as the integration and optimization of self-powered sensing systems.

XINYU MA (Student Member, IEEE) received the B.Sc. and M.Sc. degrees in electronics engineering from Mid Sweden University, Sundsvall, Sweden, in 2011 and 2014, respectively. She is currently pursuing the Ph.D. degree with the Department of Electronics Design, Mid Sweden University. Her research interests include ambient light energy harvesting for wireless sensor networks, and the modeling and characterization of PV systems under artificial lighting conditions.

BENGT OELMANN received the Ph.D. degree from the Royal Institute of Technology (KTH), Stockholm, Sweden, in 2000. From 1996 to 1998, he was a Senior Application-Specific Integrated Circuit Designer with Nordic Very-Large-Scale Integration, Trondheim, Norway. He is currently a Full Professor of electronics system design with Mid Sweden University, Sundsvall, Sweden. He has published over 140 peer-reviewed articles in the fields of low-power integrated circuit design, pixel-array sensor electronics, video coding, energy harvesting, and industrial electronics.